

Chemisorption energy of hydrogen on silicon surfaces

M. B. Raschke*

Max-Planck-Institut für Quantenoptik, D-85740 Garching, Germany

U. Höfer

Fachbereich Physik und Zentrum für Materialwissenschaften, Philipps-Universität, D-35032 Marburg, Germany

(Received 20 February 2001; published 20 April 2001)

The chemisorption energy of H_2 on Si(111)7×7 and Si(001)2×1 was determined from thermodynamic equilibrium experiments in an ultrahigh vacuum quartz apparatus at temperatures of 760 to 970 K. The obtained values of 1.7 ± 0.2 eV for Si(111) and 1.9 ± 0.3 eV for Si(001) correspond to Si–H bond energies of 3.1 and 3.2 eV, respectively. Hydrogen bonding with silicon surfaces is thus found to be considerably weaker than in silane molecules and homologous clusters.

DOI: 10.1103/PhysRevB.63.201303

PACS number(s): 68.35.Md, 42.65.Ky, 82.60.Cx, 68.43.–h

Hydrogen adsorption on silicon is of considerable technological relevance,^{1–3} and it has emerged as a prototype for understanding chemisorption and reaction dynamics on covalent solid surfaces.^{4–11} Despite over 40 years of intensive investigations, however, one of the most fundamental quantities characterizing that adsorption system, the Si–H bond energy E_{Si-H} on well defined single crystal surfaces, is not well known. Estimates based on the bond energies in silanes ($E_{Si-H} \approx 3.9$ eV) are inconsistent with the energy balance of most common models for hydrogen adsorption and desorption from silicon surfaces.^{7,12} The results of *ab initio* calculations vary widely ($E_{Si-H} = 2.9–3.7$ eV) depending on the theoretical approach.^{13–19} Previous attempts to determine E_{Si-H} experimentally have been restricted to surfaces of microcavities²⁰ and hydrogen bonding at defects of the Si/SiO₂ interface²¹ and yielded surprisingly low values ($E_{Si-H} \approx 2.5–2.7$ eV).

Here we report on equilibrium experiments determining the chemisorption energy of hydrogen on Si(111)7×7 and Si(001)2×1. The procedural difficulty arises from the large barriers for recombinative desorption (2.4–2.5 eV) (Ref. 22) and the small sticking coefficients for dissociative adsorption²³ of H_2/Si which require high temperatures and appreciable gas pressures to establish thermal equilibrium. This prohibits the application of the conventional isosteric heat measurement technique²⁴ and also renders the method of adsorption microcalorimetry²⁵ difficult. In the present work, a ultrahigh vacuum (UHV) quartz apparatus allowed equal gas and surface temperatures up to 1000 K. The resulting adsorption isotherms were recorded using optical second-harmonic generation (SHG) as a sensitive *in situ* monitor for hydrogen coverage compatible with arbitrary temperature and hydrogen pressure. Without any further assumptions about the adsorbate kinetics the data directly yields the isosteric heat of adsorption. The derived Si–H bond energies determined for both Si(111)7×7 and Si(001)2×1 are considerably lower than hydrogen bonding in silane molecules as well as the predictions made on the basis of cluster calculations.

Figure 1 shows a schematic of the experiment: a tube-shaped ($\varnothing = 5$ cm, $l \approx 25$ cm) quartz apparatus, with a quartz fixture for holding the silicon samples and optical windows

for the SHG experiments was surrounded by a furnace for temperature control and connected to a conventional UHV chamber for pumping and hydrogen dosing. The temperature was recorded with a NiCr/NiAl thermocouple inside the sample holder. Si(111) and Si(001) samples cut from a 10 Ω cm *n*-doped wafer were used. After bake-out at 400 °C the native oxide layer was removed by means of laser heating of the silicon crystal with a cw Nd:YLF laser. Applying a maximal power density of 500 Wcm^{-2} a surface temperature of 1300 K was reached as measured with a pyrometer. During the cleaning procedure the background pressure could be maintained below 4×10^{-10} mbar. Clean, well ordered Si(111)7×7 and Si(001)2×1 surfaces were obtained as verified by reproducing the laser cleaning procedure in the main UHV chamber and performing low-energy electron diffraction (LEED) and Auger electron spectroscopy analysis.

For the SHG measurements 1064 nm light from a *Q*-switched Nd:YAG laser (Coherent, Infinity, pulse duration 3.5 ns) was used with fluences of $\sim 50 \text{ mJ/cm}^2$ at 30 Hz repetition rate and $\sim 80 \text{ mJ/cm}^2$ at 100 Hz for Si(111) and Si(001), respectively. For Si(111) the polarizations of normal incidence pump and emitted SH radiation were chosen in

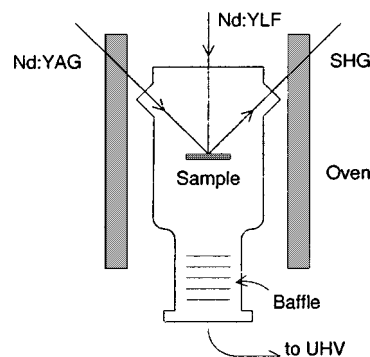


FIG. 1. Schematic of experimental setup for adsorption-equilibrium measurements. The UHV-quartz cell with the silicon sample is placed in a muffle furnace. Laser annealing (cw Nd:YLF laser) is performed for sample preparation, and second-harmonic generation (Nd:YAG laser) is used for *in situ* hydrogen coverage determination.

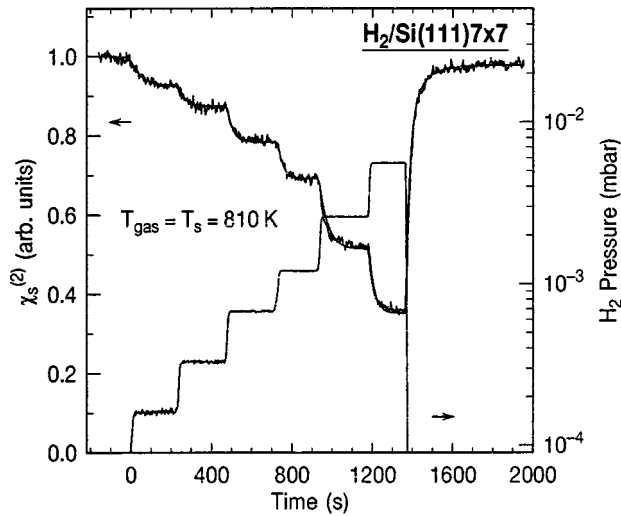


FIG. 2. Isothermal ($T=810$ K) change of the nonlinear susceptibility $\chi_{s,\xi\xi\xi}^{(2)}$ of Si(111) with hydrogen pressure. Stepwise increase of the H_2 flux leads to adjustments in the equilibrium coverage with the temporal behavior determined by the kinetics of ad- and desorption.

order to probe the anisotropic $\chi_{s,\xi\xi\xi}^{(2)}$ component of the second-order nonlinear susceptibility. For Si(001) the measurements were performed under 45° incidence and the combination of input s - and p -polarization components were chosen in order to maximize the SH signal detected without a polarizer in the exit channel. At this wavelength the resonant optical excitation of the dangling-bond-derived surface states gives rise to a high adsorbate sensitivity.⁸ The previously established relationship between nonlinear susceptibility $\chi_s^{(2)}$ and hydrogen coverage θ , $\chi_s^{(2)}(\theta) \approx \chi_{s,0}^{(2)}(1 - \alpha\theta)$, was used with $\alpha=3.1 \text{ ML}^{-1}$ for $\theta < 0.2 \text{ ML}$ in the case of Si(001) 2×1 and $\alpha=1.3 \text{ ML}^{-1}$ for $\theta < 0.4 \text{ ML}$ in the case of Si(111) 7×7 .²¹ In both cases 1 monolayer (ML) is defined with respect to the corresponding density of surface dangling bonds.

After reaching thermal equilibrium between sample and surrounding chamber walls ultrapure hydrogen gas supplied from a liquid-nitrogen cooled reservoir was introduced into the quartz cell via the main chamber where its pressure was recorded with a spinning rotor gauge. The gas thermalizes quickly and the quartz baffle in the inlet of the cell ensures separation from the gas at room temperature in the foreline. The hydrogen dissociatively adsorbs on the silicon sample and Fig. 2 shows the corresponding temporal change of the SH response from Si(111) under the isothermal conditions $T_{\text{Si}}=T_{H_2}=810$ K. The kinetics for adsorption and desorption determines the time required for the system to adjust to its equilibrium coverage. The pressure was increased in steps for low temperatures or slowly ramped up continuously in measurements at higher temperatures. The reaction is fully reversible and the desorption behavior determined after the hydrogen flux is turned off was found to be in agreement with the desorption kinetics derived in previous experiments.²² The sticking coefficients were found to be about a factor of 5 to 10 higher compared to the experiments

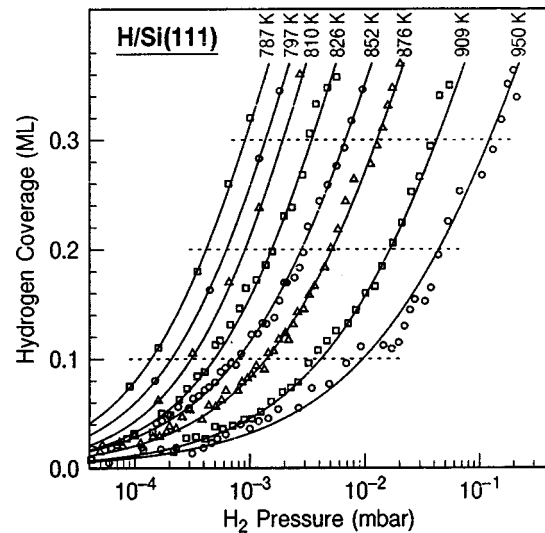


FIG. 3. Representative adsorption isotherms for hydrogen into the monohydride Si-H state on Si(111) 7×7 for different temperatures. Discrete values for hydrogen coverage and their corresponding pressure were obtained for $T=787$ K, 797 K, and 810 K from those and similar data as the ones shown in Fig. 1. For $T \geq 826$ K, data were acquired by slowly increasing the hydrogen pressure while monitoring the SH response. The solid lines serve as a guide to the eye.

having used gas at 300 K as a consequence of the higher mean translational energy. Their increase from about 10^{-5} to 10^{-6} in the investigated temperature range from 760 K to 970 K is compatible with the previous results.²³ This consistency of both the adsorption and desorption kinetics as well as the total SH response of the surface with preceding works assures cleanliness of the silicon under the present experimental conditions. Signs of surface contamination, most likely caused by interdiffusion of oxygen through the quartz walls, were only observed for temperatures in excess of 1000 K.

The adsorption isotherms obtained after conversion of the SH response to coverage are shown in Fig. 3 for different temperatures. From a series of these adsorption isotherms the isosteric heat of adsorption q_{st} can be derived evaluating the Clausius-Clapeyron equation $\partial p / \partial T|_{\theta} = q_{\text{st}} / TV_{\text{gas}}$.²⁴ For that purpose data pairs of temperature T and corresponding hydrogen pressure p leading to a constant surface coverage were taken from the results shown in Fig. 3 as well as other isotherms and are plotted in Fig. 4 (top) in the form of an isosteric plot from some representative coverage values. Rewriting the equation in the form

$$\left. \frac{\partial \ln p}{\partial(1/T)} \right|_{\theta} = - \frac{q_{\text{st}}}{k_B} \quad (1)$$

the slopes of these curves directly yield the isosteric heat of adsorption. Applying a similar procedure as described above for Si(111), corresponding data for Si(001) were obtained and are shown in Fig. 4 (bottom).

The resulting values for the isosteric heat of adsorption for both surface orientations are summarized in Table I. Af-

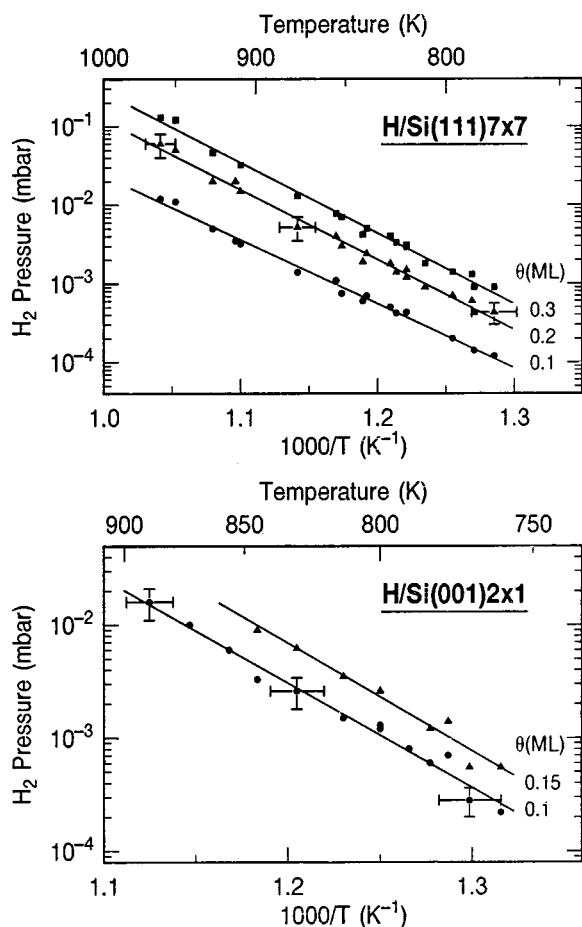


FIG. 4. Isosteric plot for different hydrogen coverages for Si(111) (top) and Si(001) (bottom). The larger uncertainties in the Si(001) data are due to a reduced SH sensitivity compared to Si(111). The solid lines represent numerical fits to the Clausius-Clapeyron equation to derive the isosteric heat of adsorption.

ter an initial increase, for coverages $\theta > 0.1$ ML the values saturate at about $(1.7\text{--}1.8) \pm 0.1$ eV for Si(111) and $(1.9\text{--}2.0) \pm 0.2$ eV for Si(001), respectively. The error bars for q_{st} are mainly due to the finite temperature range covered by the isosteric plot.

The isosteric heat of adsorption is equivalent to the chemisorption energy, i.e., the total energy change resulting from the dissociative adsorption. It thus relates to the Si-H bond energy by $2E_{\text{Si-H}} - \epsilon = q_{st} + E_{\text{H-H}}$ where ϵ includes the

TABLE I. Isosteric heat of adsorption q_{st} for hydrogen on Si(111)7 \times 7 and Si(001)2 \times 1 derived for different equilibrium surface coverages. The corresponding individual Si-H bond energies are estimated as $E_{\text{Si-H}} = 1/2(q_{st} + E_{\text{H-H}})$ with $E_{\text{H-H}} = 4.5$ eV.

θ (ML)	Si(111)7 \times 7		Si(001)2 \times 1	
	q_{st} (eV)	$E_{\text{Si-H}}$ (eV)	q_{st} (eV)	$E_{\text{Si-H}}$ (eV)
0.1	1.52 ± 0.15	3.01	1.83 ± 0.2	3.17
0.15	1.72 ± 0.15	3.11	1.9 ± 0.25	3.20
0.2	1.77 ± 0.1	3.14	2.0 ± 0.4	3.25
0.3	1.78 ± 0.1	3.14		

energies associated with, e.g., adsorbate-adsorbate interactions as well as adsorbate induced changes in surface structure. The approximate results for $E_{\text{Si-H}}$ given in Table I assuming $\epsilon = 0$ thus represent an upper limit for the individual bond energy and may overstate the actual value by a few tenths of an eV. The bond strengths on both Si(111) and Si(001) are thus considerably weaker than hydrogen bonding in silanes. For comparison the gas phase dissociation energies for the first Si-H bond for SiH₄ and Si₂H₆ are 3.92 eV and 3.74 eV, respectively.²⁶ It should be noted, however, that these values decrease systematically for substituted silicon atoms, reaching, e.g., 3.42 eV for (H₃Si)₃Si-H.²⁷

The complexity of the surface reconstruction of Si(111) renders a realistic theoretical treatment of this surface particularly difficult. Recently, however, using density functional theory (DFT) the 7 \times 7 unit cell has been treated self-consistently and chemisorption energies of 1.6 eV for the adatom-rest-atom pair and 2.1 eV for the adatom-corner hole pair were derived.¹³ An attractive lateral interaction energy was found, and the differences in the individual bond strength of 2.9, 3.2, and 3.5 eV for hydrogen adsorbed on the adatom, rest-atom, and corner hole sites, respectively, were attributed to the differences in local electronic structure. Similar DFT-based calculations have also been performed for Si(001)2 \times 1 resulting in values of 1.9–2.1 eV,¹⁴ 2.1 eV,¹⁵ and 2.14 eV (Ref. 16) (1.8–2.04 with zero-point correction) for the energy change associated with the chemisorption on the silicon dimers. On the contrary, *ab initio* cluster calculations predicted endothermicities of 2.43,¹⁵ 2.58 eV,¹⁸ and 2.90 eV.¹⁹ Whereas the results from the slab-based calculations both for Si(111) and Si(001) agree well within the uncertainties of our experimental values, the cluster approach clearly seems to overstate the chemisorption energy. This indicates that the bond parameters are notably affected by the relaxation of the total geometry specific to the individual adsorption site and long-range interactions. The slightly smaller energy gain associated with the adsorption of hydrogen on Si(111) versus Si(001) can qualitatively be explained by the lower surface free energy of the (111) crystallographic orientation. Therefore upon chemisorption this surface can less effectively reduce its energy further.

Finally we would like to discuss implications of these results for the overall energy balance of dissociative adsorption and recombinative desorption of H₂/Si. In the case of a simple one-dimensional energy diagram the heat of adsorption q_{st} , equivalent to the reaction enthalpy ΔH_r , would correspond to the difference between the activation energies for desorption and adsorption, $q_{st} = \Delta H_r = E_d - E_a$. However, for multidimensional potential energy surfaces the additional lattice degrees of freedom allow for partial energy accommodations in lattice distortions.⁸ In the case of silicon these distortions could be both quasistatic due to, e.g., already adsorbed hydrogen atoms and due to transient lattice excitations in the transition state. From kinetic measurements the barrier heights for desorption were determined to be 2.40 ± 0.1 eV and 2.48 ± 0.1 eV for Si(111) and Si(001), respectively,²² which, from comparison with the chemisorption energy values, allow for a sizeable barrier for adsorption. For the dissociative adsorption, barriers of 0.87 ± 0.1 eV

for Si(111) and 0.75 ± 0.1 eV for Si(001) (Ref. 21) were derived from the surface temperature dependence of the reaction, with complementary values obtained from recent molecular beam adsorption experiments.²⁸ From the observation that the chemisorption energy values would be compatible with the full size of the observed adsorption barriers one concludes that the lattice distortions are mostly transient in nature. In contrast, a static contribution [due to, e.g., symmetric dimers on Si(001)] would enter the energy balance through its effect on the adsorption barrier but would leave desorption largely unaffected.

With these values for E_d , E_a , and q_{st} from Table I the energy balance would be fulfilled for both surface orientations taking into account that the kinetic measurements were performed for coverages around 0.1 ML. The observed increase in chemisorption energy with coverage would be compatible with the findings of a corresponding decrease in effective barrier height for adsorption or increasing barriers for desorption as will be discussed elsewhere.²⁹

In contrast the energy balance would be far from fulfilled if one were to use the large bond energies from the molecular analogs and homologous clusters. Based on the covalent nature of the Si–H bond it has been argued that these systems have similar bond energies compared to hydrogen bonding

with single crystal surfaces. This discrepancy led to a long-standing debate regarding both the thermodynamics of the H_2/Si reaction system as well as the interpretation of the kinetic measurements.^{7,12,17,19}

In summary, the determination of the chemisorption energies of hydrogen with well defined single crystal silicon surfaces allowed for an independent consistency check of the results of the kinetic and dynamic investigations of this reaction system. The results can serve as a guideline for the different theoretical models that have been invoked for describing the hydrogen interaction with silicon. Comparing the different values for Si(111)7×7 and Si(001)2×1 with hydrogen bonding in silanes and Si clusters indicates that the local structural environment of the bonding Si atoms sensitively influences the Si–H bond strength.

The experimental method demonstrated here is not limited to the case of H/Si. It would also be most applicable to other strongly activated adsorbate systems where the bond energies are mostly unknown.

Valuable discussions with M. Dürr, K.-L. Kompa, and E. Pehlke as well as support by the Deutsche Forschungsgemeinschaft through SFB 338 are gratefully acknowledged.

*Present address: University of California, Berkeley, CA 94720.

¹J. M. Jasinski, B. S. Meyerson, and B. A. Scott, *Annu. Rev. Phys. Chem.* **38**, 109 (1987).

²G. W. Trucks, K. Raghavachari, G. S. Higashi, and Y. J. Chabal, *Phys. Rev. Lett.* **65**, 504 (1990).

³T.-C. Shen, C. Wang, G. C. Abeln, J. R. Tucker, J. W. Lyding, Ph. Avouris, and R. E. Walkup, *Science* **268**, 1590 (1995).

⁴J. A. Appelbaum and D. R. Hamann, in *Theory of Chemisorption, Topics in Current Physics Vol. 19*, edited by J. R. Smith (Springer, Berlin, 1980), p. 43.

⁵J. J. Boland, *Adv. Phys.* **42**, 129 (1993).

⁶H. N. Waltenburg and J. T. Yates, Jr., *Chem. Rev.* **95**, 1589 (1995).

⁷K. W. Kolasinski, *Int. J. Mod. Phys. B* **9**, 2753 (1995).

⁸U. Höfer, *Appl. Phys. A* **63**, 533 (1996).

⁹D. J. Doren, *Adv. Chem. Phys.* **95**, 1 (1996).

¹⁰F. M. Zimmermann and X. Pai, *Phys. Rev. Lett.* **85**, 618 (2000).

¹¹M. B. Raschke, *Elementary Surface Reactions of Hydrogen and Oxygen on Silicon: An Optical Second-Harmonic Investigation* (Herbert Utz Verlag, München, 1999).

¹²K. Sinniah, M. G. Sherman, L. B. Lewis, W. H. Weinberg, J. T. Yates, Jr., and K. C. Janda, *Phys. Rev. Lett.* **62**, 567 (1989); *J. Chem. Phys.* **92**, 5700 (1990).

¹³H. Lim, K. Cho, I. Park, J. D. Joannopoulos, and E. Kaxiras, *Phys. Rev. B* **52**, 17 231 (1995); K. Cho, E. Kaxiras, and J. D. Joannopoulos, *Phys. Rev. Lett.* **79**, 5078 (1997).

¹⁴A. Vittadini and A. Selloni, *Chem. Phys. Lett.* **235**, 334 (1995).

¹⁵E. Pehlke and M. Scheffler, *Phys. Rev. Lett.* **74**, 952 (1995).

¹⁶P. Kratzer, B. Hammer, and J. K. Nørskov, *Phys. Rev. B* **51**, 13 432 (1995).

¹⁷P. Nachtigall, K. D. Jordan, and C. Sosa, *J. Chem. Phys.* **101**, 8073 (1994).

¹⁸Z. Jing and J. L. Whitten, *J. Chem. Phys.* **102**, 3867 (1995).

¹⁹M. R. Radeke and E. A. Carter, *Phys. Rev. B* **54**, 11 803 (1996).

²⁰S. M. Myers, D. M. Follstaedt, H. J. Stein, and W. R. Wampler, *Phys. Rev. B* **45**, 3914 (1992); W. R. Wampler, S. M. Myers, and D. M. Follstaedt, *ibid.* **48**, 4492 (1993).

²¹K. L. Brower and S. M. Myers, *Appl. Phys. Lett.* **57**, 162 (1990).

²²M. L. Wise, B. G. Koehler, P. Gupta, P. A. Coon, and S. M. George, *Surf. Sci.* **258**, 166 (1991); G. A. Reider, U. Höfer, and T. F. Heinz, *J. Chem. Phys.* **95**, 4080 (1991); U. Höfer, Leping Li, and T. F. Heinz, *Phys. Rev. B* **45**, 9485 (1992).

²³P. Bratu and U. Höfer, *Phys. Rev. Lett.* **74**, 1625 (1995); P. Bratu, K. L. Kompa, and U. Höfer, *Chem. Phys. Lett.* **251**, 1 (1996).

²⁴K. Christmann, *Introduction to Surface Physical Chemistry* (Springer, New York, 1991).

²⁵D. A. King, *Chem. Rev.* **98**, 797 (1998).

²⁶R. Walsh, *Acc. Chem. Res.* **14**, 246 (1981).

²⁷S. Pai and D. Doren, *J. Phys. Chem.* **98**, 4422 (1994).

²⁸M. Dürr, M. B. Raschke, and U. Höfer, *J. Chem. Phys.* **111**, 10 411 (1999).

²⁹M. B. Raschke and U. Höfer (unpublished). Microscopically both attractive lateral dangling bond interactions (Refs. 5 and 8) as well as adsorbate induced relaxations of the local surface geometry (Ref. 12) can account for the apparent in q_{st} . However, possible nonequilibrium effects cannot be excluded for the low coverage limit.